



THEME SECTION

# Harbour seal spatial distribution estimated from Argos satellite telemetry: overcoming positioning errors

Jakob Tougaard<sup>1,\*</sup>, Jonas Teilmann<sup>1</sup>, Svend Tougaard<sup>2</sup>

<sup>1</sup>National Environmental Research Institute, University of Aarhus, Department of Arctic Environment, Frederiksborgvej 399, PO Box 358, 4000 Roskilde, Denmark

<sup>2</sup>Fisheries and Maritime Museum, Tarpbagevej 2, 6710 Esbjerg V, Denmark

**ABSTRACT:** A limiting factor of satellite telemetry in the context of habitat use by marine mammals is the low accuracy of the received positions. A novel statistical analysis to overcome the low accuracy was developed in the context of processing data on harbour seals *Phoca vitulina* for the atlas of Danish mammals. Ten harbour seals were caught in the Danish Wadden Sea and tracked with satellite transmitters. The statistical analysis reversed the problem of positioning: Instead of attempting to correctly assign each individual position to a single grid cell, our approach considers the combined probability that at least one position originated in each grid cell. Thus, all satellite-derived positions, including positions of poor precision, can contribute to the evaluation. The method is an alternative to other methods describing spatial use, such as kernel home range, and constitutes a viable approach for inclusion of satellite-derived positional data into spatial modeling of animal distribution and habitat use.

**KEY WORDS:** Service Argos · Positioning accuracy · Grid survey · Abundance · Kernel home range · *Phoca vitulina* · North Sea · Spatial modelling

—Resale or republication not permitted without written consent of the publisher—

## INTRODUCTION

It is notoriously difficult to estimate the spatial distribution of marine mammals. Marine mammals at sea are hard to discern, and species determination is often difficult, even for trained observers. However, the situation has changed considerably with the introduction of satellite-linked telemetry. Satellite telemetry has inherent limitations, such as low accuracy in positioning of marine mammals. Marine mammals are most often tracked by the Argos satellite system (e.g. Stewart et al. 1989, Teilmann et al. 1999, Laidre et al. 2002). Argos positions have variable accuracy, and the distance from the calculated to the true position ranges from a few hundred metres to more than 50 km (Vincent et al. 2002, White & Sjöberg 2002). These positioning errors can affect conclusions to various degrees, depending on the behaviour of the species tagged and the specific

questions addressed. In studies of off-shore species that migrate 100s to 1000s of km, a low accuracy may not be critical to determining spatial distribution and area use. In contrast, determination of the distribution and area use of species that move over short distances within complex habitats is almost always limited by the accuracy in positioning. Area use is commonly described by estimating the home range of the animal. Home range can be expressed in various ways, such as fixed kernels (e.g. Worton 1989, Seaman & Powell 1996, Born et al. 2004) or minimum convex polygons (Mohr 1947). Other models of spatial use also take advantage of *a priori* knowledge of the behaviour of the species, obtained by other means (e.g. VHF-telemetry and aerial counts at haulout sites; Matthiopoulos 2003).

This study presents a new strategy, originally developed for compilation of data for the atlas of Danish mammals (Baagøe & Jensen 2007) but with consider-

\*Email: jat@dmu.dk

able potential in the context of spatial modelling of species' distribution. The method uses available information on the precision of all positions, including those of low precision, obtained by analysing all positions as a whole together with a measure of their individual precision. This makes it possible to identify those grid cells most likely to have been visited by at least 1 animal. The distribution range achieved is thus conservative, in the sense that only areas with high confidence of animal presence are included.

## MATERIALS AND METHODS

**Tagging of animals.** Ten harbour seals *Phoca vitulina* (5 males, 5 females) of different age classes (Table 1) were equipped with Argos satellite transmitters (SDR-T16 with 4 flat M1 batteries, Wildlife Computers). Animals were caught on Rømø Island in the Danish Wadden Sea on 3 separate occasions in the first half of 2002 and transmitters were glued to the fur on the top of the head with fast hardening epoxy glue (Araldite 2012). Transmitters transmitted daily with a maximum of 500 uplinks allowed per day and were prevented from transmitting during the night hours (22:00 to 03:00 h local time) when satellite coverage was poor. Median transmission time was 77 d (range 49 to 100 d) and a median of 3.8 positions per day per transmitter was acquired (range 1.5 to 4.6 d<sup>-1</sup>). Thirteen percent of the positions belonged to Location classes 1 to 3 (most precise); the remaining were 0, A and B (least precise). See Tougaard et al. (2003) for additional information on capture and tagging. Capture and tagging of animals was carried out with permission from the Danish Ministry of Environment, Forest and Nature Agency.

**Use of positions in the atlas of Danish mammals.** The atlas of Danish mammals (Baagøe & Jensen 2007) compiles all recent verified observations of mammals on Danish territory (including the exclusive economic zones, EEZ), separated into 10 × 10 km Universal Transverse Mercator (UTM) grid cells. The fundamental logic of the atlas is simple: only grid cells with verified observations of a particular species are to be included as positive, and thus presence but not density is assigned to

the grid cells. As there are very few verified observations of seals from the open sea, it was suggested that the available satellite telemetry data be included, even though the precision of most of the Argos positions was of the order of several km. The precision of most observations was not sufficient to assign them with certainty to a particular 10 × 10 km grid cell. The challenge then was to rephrase the presence/absence question of the grid survey in statistical terms and identify cells as positive for presence when the likelihood that at least 1 seal is present is above a predetermined criterion. One example is shown in Fig. 1, which illustrates a section of 15 UTM grid cells with positions received from 10 harbour seals. The question is: Which cells are to be counted as positive for presence (at least 1 observation of a seal) and which are not? Cells to the NW are clearly empty and cells LH40, LH51 and LH61 are likely to be positive, but the status of the others is less clear.

Table 1. *Phoca vitulina*. Details of the tagged harbour seals. Positions transmitted by Argos satellite transmitter

No.	Sex	Weight (kg)	Length (cm)	Date tagged (yy/mm/dd)	No. of transmission days	No. of positions
1	M	33	141	02/01/04	84	255
2	F	24	107	02/01/04	75	344
3	F	26	111	02/01/04	81	305
4	M	25	116	02/01/04	69	227
5	M	110	172	02/02/18	92	336
6	F	43	143	02/02/18	78	355
7	M	110	164	02/02/18	100	154
8	F	44	134	02/05/06	50	114
9	M	47	139	02/05/06	62	280
10	F	52	150	02/05/06	49	208

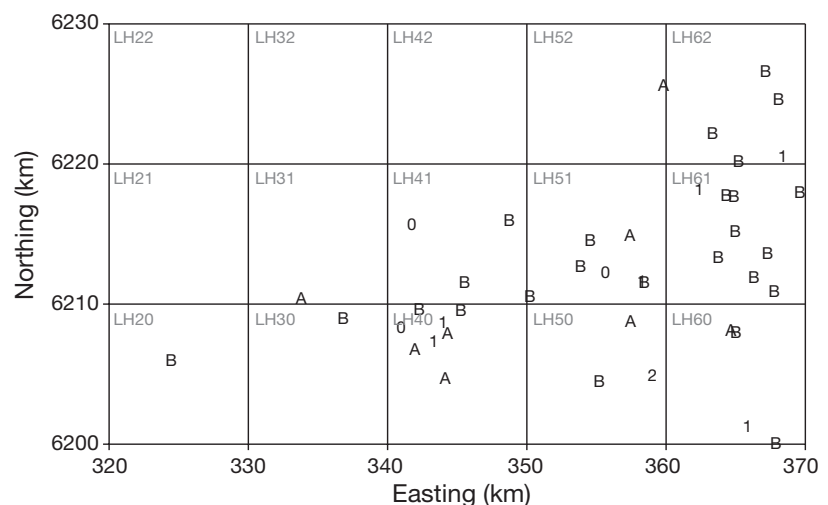


Fig. 1. Example of Argos positions received from 3 harbour seals in the North Sea. Shown are 15 Universal Transverse Mercator squares (each 10 × 10 km) from the central part of the Danish North Sea. Received positions of the tagged harbour seals are indicated with letters or numbers corresponding to their precision (Location class, see Table 2)

The simplest solution to the problem is to include only positions with high precision (Location class 1 to 3; 68% error percentile 1000 m or less, see 'Model' below). However, a substantial amount of information is lost this way (87% of all positions in the present study would be discarded); neither does this solve the problem for positions located close to grid cell borders, where there may be a considerable likelihood that the true position was located in the adjacent square.

**Model.** Based on the number of uplinks received by a single satellite during a single passage and on the internal consistency of the solutions from the positioning algorithms, each Argos position is assigned by Service Argos to 1 of 6 precision classes: B, A, 0, 1, 2 and 3 (Keating 1994). Location class B contains the least precise positions and Location class 3 the most precise positions. Service Argos only specifies the precision of the three best location classes (Location classes 1 to 3). Errors are given as 68% percentiles on longitude and latitude. The 68% percentile for Location class 3 is 150 m, indicating that the reported longitude is within 150 m from the true longitude for 68% of the positions and likewise for latitude. This result is not equivalent to 68% of the positions being within 150 m of the true position, as errors on longitude and latitude are independent of one another. The fraction of positions within 150 m of the true position is significantly smaller, below 40%. The positioning errors (expressed as 68% percentiles) for all 6 location classes were determined empirically by Vincent et al. (2002), see our Table 2. Note that Location class A is considerably more accurate than Location class 0 and comparable to Location class 1.

We used the values measured by Vincent et al. (2002) below, including their results for Location class 1 to 3, even though their estimates are not identical to those supplied by Service Argos. Vincent et al. (2002) used transmitters with comparable specifications to those used in our study and deployed in a similar

fashion (glued onto the fur of unrestrained grey seals held in captivity). We used the error estimates by Vincent et al. (2002), but it would also be feasible to use other error estimates, if such exist and are considered more appropriate for other applications.

Following Vincent et al. (2002), we filtered the data to remove extreme positions using a SAS-program (Argos\_Filter V 7.01; prepared by Dave Douglas, USGS, Alaska Science Center). The program identifies outlying positions based on a maximum swimming speed between positions (McConnell et al. 1992) and angle between straight-line paths connecting 3 consecutive positions (Keating 1994). The threshold values were a maximum swimming speed of  $2.7 \text{ m s}^{-1}$  (McConnell et al. 1992) and minimum angle of  $10^\circ$ . After filtering, it was assumed that the errors in latitude and longitude were normally distributed according to a bivariate Gaussian distribution. The bivariate Gaussian distribution has the parameters  $\mu_x$  and  $\mu_y$  (mean error on longitude and latitude, respectively),  $\sigma_x$  and  $\sigma_y$  (standard deviation of errors) and  $\rho$  (correlation between errors on longitude and latitude). We further assumed that errors in longitude and latitude were uncorrelated ( $\rho = 0$ ) and that mean errors were zero (no systematic bias in observed positions towards any particular direction). These assumptions are all supported by the results of Vincent et al. (2002).

The probability that the true position associated with a given observed position is located inside a given rectangle was assumed to depend on the distance between the observed position and the centre of the rectangle as well as the size of the rectangle. The probability that the true position of a seal is inside a particular  $10 \times 10 \text{ km}$  UTM square is calculated on the basis of the cumulated bivariate Gaussian distribution (Eq. A4; see also Fig. 2. Probabilities are shown as a function of the distance between the centre of the square and the position reported by Service Argos (referred to hereafter as 'observed position'). For the good location classes (A, and 1 to 3) there is a very high likelihood that the seal was in fact inside the square of the observed position, unless the observed position was within 1000 m of the border of the square. For Location classes 0 and B there is a significant probability that the true location was located in one of the adjacent squares, even if the observed position was located in the centre of the square (probability of the true position being in an adjacent square is 0.10 and 0.38 for Location class 0 and B, respectively).

The measure we are seeking is the combined probability that at least 1 true position ( $n$ ) was located inside a given square ( $A$ ),  $P(n_A > 0)$ .  $P(n_A > 0)$  is calculated from the probability that each individual position belongs inside the square, both for observed positions inside the square and in adjacent squares.

Table 2. 68% percentiles for difference between true and calculated position for each of the 6 location classes (for details see 'Materials and methods; Model'). Nominal values provided by System Argos, and empirically determined errors from Vincent et al. (2002) are shown. -: no data available; long.: longitude; lat.: latitude

Location class	Service Argos long. and lat. (m)	Vincent et al. (2002)	
		Long. (m)	Lat. (m)
3	150	295	157
2	350	485	259
1	1000	1021	427
0	-	3029	1851
A	-	909	678
B	-	4815	3193

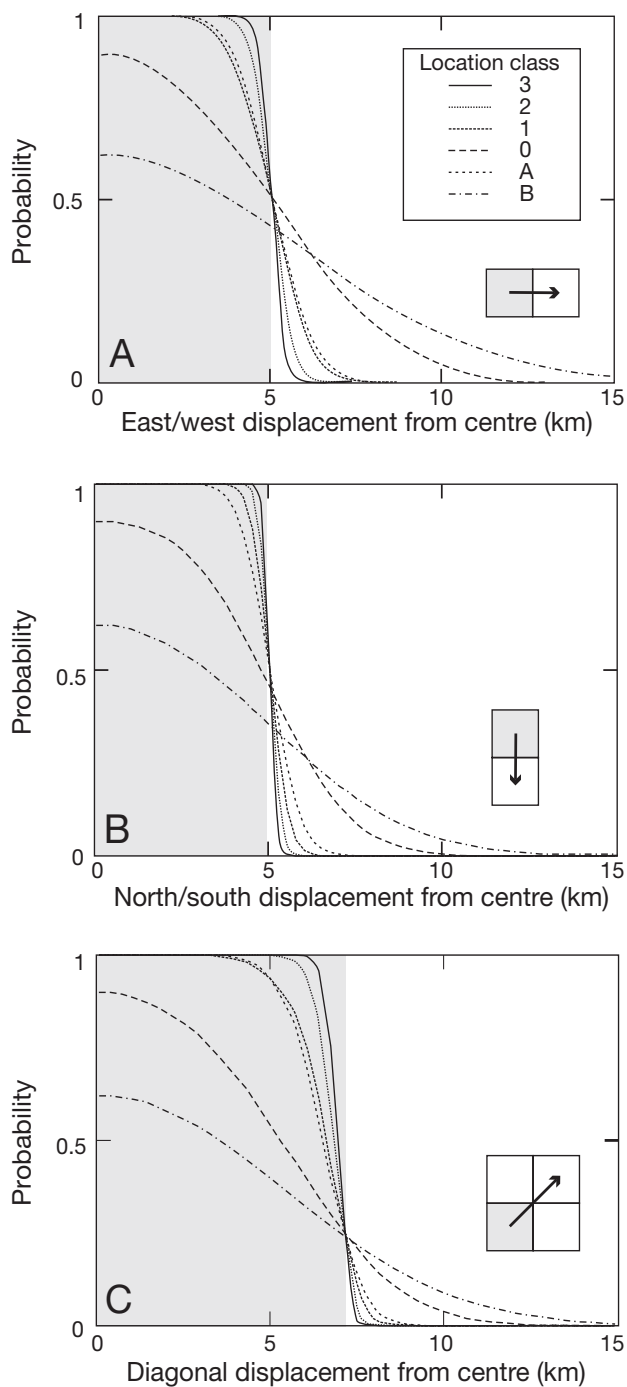


Fig. 2. Calculated probability that the true position of the transmitter associated with a particular position provided by Service Argos belongs inside a 10 × 10 km Universal Transverse Mercator (UTM) square as a function of the distance between the centre of the square and the observed position. (A) Displacement in longitude, (B) displacement in latitude and (C) displacement along the diagonal. Inside the grey rectangle the position reported by Service Argos is located in the UTM square being evaluated; in the white rectangle the observed position is in the adjacent square. Small insert shows direction of displacement from centre of the grey square. See Table 2 for location class

$$P(n_A > 0) = 1 - P(n_A = 0) = 1 - \prod_{i=1}^N [1 - P(v_i \in A)] \quad (1)$$

$P(n_A > 0)$  is calculated as 1 minus the probability that no uplinks originated from the square (A). The probability that no uplinks came from A is again calculated as the product of the  $N$  probabilities that each of the  $N$  individually observed positions did *not* originate in the particular square,  $1 - P(v_i \in A)$ .  $v_i$  is the  $i$ th position in the dataset, which contains a total of  $N$  positions, and  $n_A$  is the number of true positions inside square A.

Consider as an example Square LH41 in Fig. 1. LH41 contains 1 position of Location class 0 and 2 positions of Location class B. Fig. 3 shows the total probability that at least 1 of these 3 positions originated from Square LH41 ( $p = 0.922$ ), as well as the probability for each adjacent square that at least 1 of the positions observed inside the adjacent squares belonged in LH41. There is more than 50% chance that at least 1 of the positions in LH40 originated in LH41 and the same is true for Square LH51. If all positions in the 9 squares are included in the calculation, the total probability that at least 1 position had its true origin inside LH41 becomes:  $p(n_{LH41} > 0) = 0.985$ . In other words: the probability that at least 1 seal visited LH41 and transmitted signals while there is 98.5%.

A second parameter that can be associated with each UTM-square is the most likely number of true positions

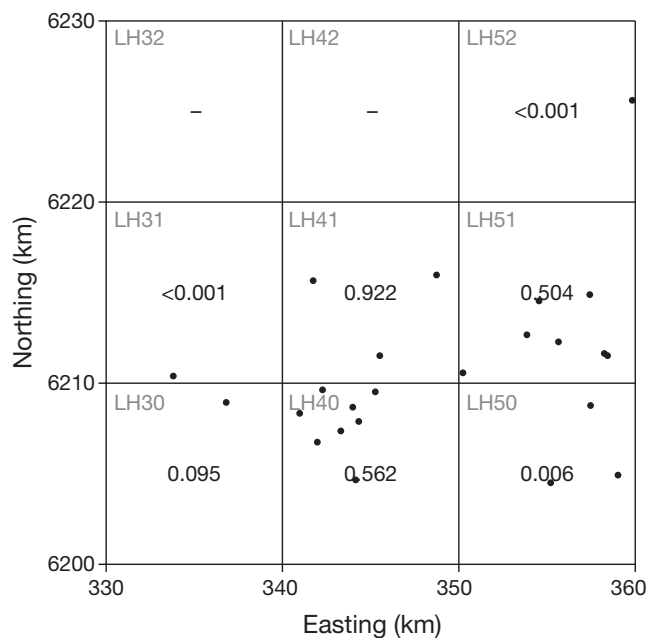


Fig. 3. Evaluation of Universal Transverse Mercator (UTM) 10 × 10 km Square LH41 and adjacent squares. The probability that at least 1 of the positions inside each square belongs in LH41 is calculated; see Appendix 1 for details on calculation. No probabilities assigned to LH32 and LH42 as they contained no observed positions. Individual positions are indicated by black dots

inside the square,  $E(n_A)$ . This is given as the sum of the individual probabilities associated with individual observations:

$$E(n_A) = \sum_{i=1}^N P(v_i \in A) \quad (2)$$

Thus  $E(n_A)$  is found for square  $A$  as the sum of the individual probabilities that the  $i$ th position  $v_i$  truly belongs in the square, summed over all  $N$  positions of the dataset.  $E(n_A)$  thus represents the expected average number of positions in the square in the entirely hypothetical situation where all positions could be recalculated based on the same number of uplinks from the same true positions. In other words,  $E(n_A)$  is the best estimate of the number of true positions in the square.

**Practical considerations.** Service Argos supplies positions in degrees longitude and latitude and they must be converted to UTM coordinates by an appropriate transformation, provided by GIS-software.  $P(n_A > 0)$  and  $E(n_A)$  can then be calculated square by square from Eqs. (A5) to (7). Positions may cover more than 1 UTM zone, in which case calculations must be performed separately for each of the zones covered, with a sufficiently large overlap. Difficulties arise where 2 UTM zones meet, as the squares are no longer true squares but trapezoids and of unequal size. As Eq. (A5) can only handle rectangles, some approximation using smaller rectangles must be made. In our study, most positions were located in UTM Zone 32N, with the remaining positions in the eastern part of Zone 31N. The overlap of positions into Zone 31N was considered sufficiently small to justify a westward extension of Zone 32 to contain all positions.

Eqs. (A5) & (7) include all positions in the dataset in calculation of  $P(n_A > 0)$  and  $E(n_A)$  for every grid cell. Calculations can be drastically reduced if more remote positions are excluded. Fig. 2 shows that separation between observed and true position very rarely exceeds 15 km. This implies that for all practical purposes, the true position is either located in the same square as the observed position or in one of the 8 immediately adjacent squares, reducing computations considerably. It also implies that if a square is empty and surrounded by only empty squares then both  $P(n_A > 0)$  and  $E(n_A)$  can be set to zero for all practical purposes.

The size of the grid cells was set at  $10 \times 10$  km but both larger and smaller cell sizes can be used. Smaller cells, down to  $4 \times 4$  km have been used with good results for smaller subsamples of the dataset. Decreasing cell size beyond this will not give increased resolution, as resolution then becomes limited by the positioning errors.

Positions on or close to land pose a separate problem. Positions on land should definitely be included in the analysis if they are no more than 10 km from the shore.

In fact, observed positions in squares completely covered by land should add more weight to the nearest square containing shoreline, as we know with certainty that the true position was not in the square of the observed position. Such a correction has not been attempted here as it is not trivial and it was considered that it would add little to the quality of the results. It may however, significantly improve the quality of the results in other locations, e.g. where animals are swimming in narrow waters between larger islands or peninsulas.

If results are used in an atlas survey for which the method was developed, a criterion for when to include cells as positive for presence is required. A criterion of 95% probability was used for the atlas of Danish mammals, i.e. all  $10 \times 10$  km grid cells with a value of  $P(n_A > 0)$  larger than 0.95 was counted as positive for presence.

## RESULTS

Fig. 4A shows all positions of the dataset in the German Bight and central North Sea, together with highlighting of  $10 \times 10$  km UTM squares which contained one or more high-precision positions (Location class 1, 2 or 3). This map clearly illustrates the large amount of information lost if low precision positions are excluded from analysis.

Fig. 4B shows UTM squares coloured according to the value of  $P(n_A > 0)$ . This map expresses the likelihood that one or more of the tagged seals visited the individual squares, and thus reflects the area used by the seals in the period the transmitters were active.

A large clustering of squares with very high probabilities of presence is found around the tagging site and to the north and west of the site. Numerous positions were received from this area, which contains important haulout sites and likely also foraging areas. High probability squares are also found further offshore, reflecting the fact that several of the individual seals ventured out in a north-western direction to the central North Sea and spent considerable time at more or less the same position, presumably foraging, before they found a different site or returned to the haulout sites in the Wadden Sea. One seal swam to the Netherlands and spent more than 1 mo around the island of Terchelling, which is also reflected in high probability squares in this area.

Values of  $E(n_A)$  for UTM squares in the German Bight and central North Sea are shown in Fig. 4C. This map represents the density of true positions and is thus a reflection of where the seals spent most of their time, although the probability of receiving locations may be influenced by differences in the surface behaviour of the seals among the different areas.

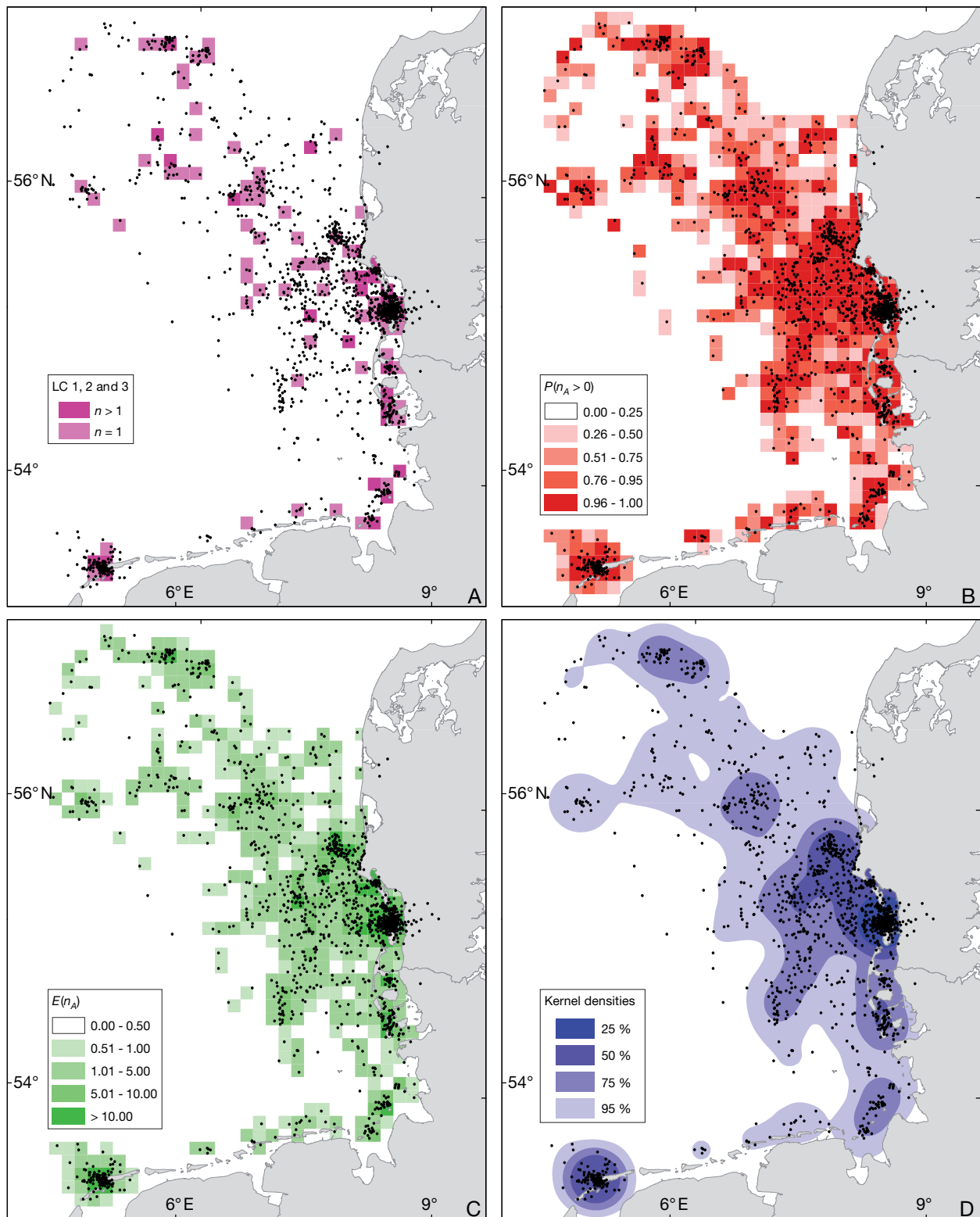


Fig. 4. Satellite-derived positions of 10 harbour seals tracked in 2002 (indicated by black dots). (A) Universal Transverse Mercator (UTM) squares ( $10 \times 10$  km, Zone 32N) with high precision positions (LC, Location class 1, 2 or 3, see 'Materials and methods'); (B) UTM squares with high probabilities of at least 1 true position ( $n$ ) being inside a square ( $P(n_A > 0)$ ); (C) UTM squares with high expected number of true positions ( $E(n_A)$ ); (D) Fixed kernel probabilities calculated from all positions calculated in ArcGIS animal movement module, quartic kernels, scaling factor  $10^6$  and smoothing factor  $3 \times 10^5$ . See 'Results' for further explanation

Squares around the tagging site and other haulout sites have very high values of  $E(n_A)$ , due to the large number of uplinks received from these areas. This result reflects the fact that the seals clustered on a limited number of sites during haulout, whereas they distributed more widely during offshore foraging. An additional factor is that transmission conditions are more favourable when the animals are on land or in shallow water (i.e. the transmitter is out of the water more often). Nevertheless, there are several clusters of positions in the open sea where  $E(n_A)$  is considerably higher than 1, indicating that these areas were used extensively by 1 seal or more.

For comparison, contours of fixed kernels calculated from the same dataset are shown in Fig. 4D. The 25% kernel density contour estimates the smallest area containing 25% of the positions and similarly for the 50, 75 and 95% contours.

## DISCUSSION

The method presented here for analysing Argos positional data was developed for a specific purpose, namely the collection of verified observations of seals in connection with an atlas survey. For this purpose, the method worked very well. The method is simple and no assumptions regarding the behaviour of the tagged animals are needed for the evaluation.

The method has potential value in other types of studies, as in the context of evaluating effects of man-made or natural structures on animal distribution, such as whether animals pass under bridges, through narrow straits or canals or spend time inside well defined areas such as large harbours, offshore wind farms or marine protected areas. In the absence of other data such as visual sightings, Argos positions, even of poor precision classes, can thus help provide answers to the question: Do we have any evidence that species A has ever been present in this particular area of interest? The method may even be applicable to other types of inaccurate positional data where the precision of each position is known, such as those obtained by acoustic positioning of sound sources (e.g. Wahlberg et al. 2001).

As stated in the 'Introduction', Argos based telemetry systems are excellent for large-scale tracking of marine mammals, but at smaller scales the precision of positions is often too low to allow for strong conclusions on the exact location of the tagged animal. Problems are exacerbated by the fact that most positions received from transmitters on marine mammals are based on very few uplinks and are consequently of low precision. Statistical methods are often needed in order to interpret results at scales of 10 km and less. The method presented in this paper represents one

such approach, aimed at a very well-defined problem: How likely is it that tagged animals visited one or more particular areas? This goal was achieved by providing an objective method for evaluating Argos positioning data in a  $10 \times 10$  km UTM grid. There are fundamental limitations of the Argos system, however, which are not easy to overcome. One such limitation is that calculations are based on uplinks, which are highly irregularly spaced in time as they are neither transmitted nor received at regular intervals. Transmission rate is affected by the behaviour of the animal and reception is determined by time of satellite passages, as well as other factors such as waves and nearby high land that can obstruct the line of sight to satellites. Thus, the maps produced by a simple analysis of the positions, such as in the present study, must not be interpreted directly in terms of animal densities or probability of presence. Strictly speaking, the maps only express uplink probabilities. That positions are concentrated around a few haulout sites is not only due to the 10 tagged seals converging on these sites, but also to the fact that the likelihood of receiving a position from these areas is very high, as haulout behaviour and swimming in shallow water favour transmission.

The most important limitation of the Argos positions regards absence data, which in part results from the uneven distribution of positions in time. Thus, we cannot strictly know whether empty areas were visited by the seals or not. The problem is evident in Fig. 4B,C where empty squares are found among visited squares, as e.g. in the Dutch Wadden Sea and the western part of the study area. In cases where we know that the seals must have passed through these areas, we have no way of determining what route they took. Addressing this would require that positions are evaluated as sequences and not individually. It is possible to do this, but at the cost of introducing a number of variables describing the statistics of animal movement (e.g. average and maximum swimming speed, directionality of movement). As the average swimming behaviour of the animals is likely to change, depending on the activity of the animal (foraging, travelling or hauling out), a considerably more complex model would be the result, relying on many critical assumptions and hence higher uncertainty in the results.

### Comparison to kernel density estimates

The present method of evaluating ARGOS positional data has some resemblance to maps of kernel density estimates (e.g. Worton 1989, Seaman & Powell 1996; see also our Fig. 4D) as they both evaluate the tagged animals' use of the area by assessing probabilities of presence. There are important differences, however.

First of all, a kernel density analysis assumes that all positions are accurate, which is not correct. Ignoring the inaccuracy of positions is likely to result in an over-estimation of home range sizes, especially when analysing at smaller scales. For example, consider the case where an animal remains at the same spot for a long time (e.g. during haulout). Received positions will be distributed around this fixed true position and may easily show an inaccuracy of several km due to the uncertainty in the Argos positioning, resulting in a considerable kernel area, although the animal did not move at all. Thus, caution should be exercised when evaluating kernel density estimates on scales comparable to the size of the positioning errors.

Likewise, the present method cannot overcome the inaccuracy of the positions. There is also a limit to the resolution with which data can be analysed in a meaningful way. As resolution is increased, by evaluating smaller and smaller squares, the probabilities assigned to the individual squares also become smaller and smaller, and at a resolution roughly equivalent to the magnitude of the errors (i.e. a few km) nothing further is gained by decreasing the size of the squares, except a dramatic increase in computation time.

A more fundamental difference between kernel density estimates and the present analysis is the smoothing involved in computation of kernel densities. Kernel density maps are created by the summation of a large number of smaller kernels each centred on 1 satellite position and all of the same size. The size of this fundamental kernel is a determining factor for the outcome of the final result, and changing this value, sometimes termed 'smoothing factor' will critically influence the resulting contours. A few scattered positions and a high smoothing factor will often result in contiguous kernel density contours that contain all positions, as well as a great deal of the surroundings. This approach can result in misleading conclusions, unless these limitations are kept in mind. As an example, consider a few positions evenly spaced more or less along a straight line, a pattern often seen for marine mammals moving from one area to another. A kernel density estimate based on these positions and a high smoothing factor will tend to result in an oval shaped surface, which may extend many km to the sides of the track. Thus, although we have good reason to believe that the animal moved in a straight line, a kernel density analysis would suggest that there was a significant probability that the animal could be found far to the sides of the track.

A low smoothing factor, on the other hand, will often result in maps with many non-contiguous kernel density contours, each containing only a few or even only 1 position. Picking an appropriate amount of smoothing is thus critical to the final result of the analysis.

No smoothing factor is included in the new grid-based method presented here, and areas with few or no positions will always result in low probability of presence. In some cases, such as in an atlas survey, this is a considerable strength of the method, compared to kernel density maps, as no parameters other than precision of the satellite positions are needed for the analysis. For other applications, some degree of smoothing may in fact be desirable, in which case kernel density maps should be favoured. Thus, it is not appropriate to generalise about whether kernel home ranges or the present grid analysis is superior. Results from both methods should be interpreted carefully and cautiously, especially on fine scales. For some applications, they may supplement each other well. However, one case, in addition to the atlas survey, where the present method seems considerably more appropriate than kernel density estimates is in spatial modelling of animal distribution.

### Spatial modelling

Spatial modelling has become a central tool in the description of animal distribution in space (e.g. Elith et al. 2006, Redfern et al. 2006). In general terms, spatial modelling is a set of statistical techniques used to correlate observations of animals in space with a range of environmental predictors, whereby otherwise hidden relationships between predictors and animal occurrence can be revealed. There are several problems associated with spatial modelling, particularly when the input is positional data from satellite telemetry. However, much of the groundbreaking work in this field has been on material from museum collections. Such data suffer from some of the same weaknesses as telemetry data, such as the low number of observations, no information on absence and strong bias in sampled areas. Addressing these issues has been a central priority in the development of spatial modelling tools developed in recent years, and these models have been shown to perform well, even with strongly biased data (Elith et al. 2006).

Individual Argos positions are not particularly well suited as input for spatial modelling. Besides the problem of inaccuracy of the positions, which one can choose to ignore or solve by using the good location classes only, the main problem is how to include information on environmental conditions in areas where the animals were not seen. This can be solved by the inclusion of random sampled points from low density areas; however, this approach is unsatisfactory, as it involves subjective decisions on what areas to sample and how many absence data should be included. The grid-based approach described here represents an alternative

without the need for subjective decisions of that sort. By directly evaluating presence in grid cells instead of using the individual points, not only is the absence information included automatically, but the presence information is also supplied in a graded measure (as probabilities, or expected number of true positions), instead of the binary presence/absence data from the positions on their own. Thus, the grid analysis method provides output of a nature which can be directly entered into spatial modelling algorithms and, thus, has potential for becoming a valuable tool to determine spatial distribution from satellite-derived positions.

*Acknowledgements.* Capture and tagging of seals was done with the help of the Search and Rescue boat of Rømø Island and the project would not have been possible without the skilled assistance of the crew. Staff from the Fisheries and Maritime Museum and the National Environmental Research Institute, as well as a large number of volunteers, are acknowledged for enthusiastic participation in the field. Mary S. Wisz is thanked for fruitful discussions and suggestions regarding this manuscript. Rune Dietz, Susi Edrén and Kasper Johansen are all thanked for assisting in analysis of the data and for preparing final versions of the maps. Suggestions from 3 anonymous reviewers were helpful in improving the manuscript. The satellite telemetry study was funded by the Danish Energy Authority through contract with Elsam A/S as part of a monitoring program on seals in and around the Horns Rev Offshore Wind Farm.

#### LITERATURE CITED

- Baagøe HJ, Jensen TS (2007) Dansk pattedyratlas. Gyldendal, Copenhagen
- Born EW, Teilmann J, Aquarone M, Riget FF (2004) Habitat use of ringed seals (*Phoca hispida*) in the North Water area (north Baffin Bay). *Arctic* 57:129–142
- Divgi DR (1979) Calculation of univariate and bivariate normal probability functions. *Ann Stat* 7:903–910
- Elith J, Graham CH, Anderson RP, Dudik M and others (2006) Novel methods improve prediction of species' distribution from occurrence data. *Ecography* 29:129–151
- Keating KA (1994) An alternative index of satellite telemetry location error. *J Wildl Manag* 58:414–421
- Laidre KL, Heide-Jørgensen MP, Dietz R (2002) Diving behaviour of narwhals (*Monodon monoceros*) at two coastal localities in the Canadian High Arctic. *Can J Zool* 80: 624–635
- Matthiopoulos J (2003) Model-supervised kernel smoothing for the estimation of spatial usage. *Oikos* 102:367–377
- McConnell BJ, Chambers C, Fedak MA (1992) Foraging ecology of southern elephant seals in relation to the bathymetry and productivity of the Southern Ocean. *Antarct Sci* 4:393–398
- Mohr CO (1947) Table of equivalent populations of North American mammals. *Am Midl Nat* 37:223–249
- Redfern JV, Ferguson MC, Becker EA, Hyrenbach KD and others (2006) Techniques for cetacean-habitat modelling. *Mar Ecol Prog Ser* 310:271–295
- Seaman DE, Powell RA (1996) An evaluation of the accuracy of kernel density estimators for home range analysis. *Ecology* 77:2075–2085
- Stewart BS, Leatherwood S, Yochem PK, Heide-Jørgensen MP (1989) Harbor seal tracking and telemetry by satellite. *Mar Mamm Sci* 5:361–375
- Teilmann J, Born EW, Aquarone M (1999) Behaviour of ringed seals tagged with satellite transmitters in the North Water polynya during fast-ice formation. *Can J Zool* 77: 1934–1946
- Tougaard J, Ebbesen I, Tougaard S, Jensen T, Teilmann J (2003) Satellite tracking of harbour seals on Horns Reef. Use of the Horns Reef wind farm area and the North Sea. Report to Elsam Engineering A/S. Biological Paper no. 3, Fisheries and Maritime Museum, Esbjerg
- Vincent C, McConnell BJ, Ridoux V, Fedak MA (2002) Assessment of Argos location accuracy from satellite tags deployed on captive gray seals. *Mar Mamm Sci* 18: 156–166
- Wahlberg M, Møhl B, Madsen PT (2001) Estimating source position accuracy of data from a large aperture hydrophone array for bioacoustics. *J Acoust Soc Am* 109:397–406
- White NA, Sjöberg M (2002) Accuracy of satellite positions from free-ranging grey seals using ARGOS. *Polar Biol* 25: 629–631
- Worton BJ (1989) Kernel methods for estimating the utilization distribution in home-range studies. *Ecology* 70: 164–168

### Appendix 1. Calculation of $P(n_A > 0)$ and $E(n_A)$

Given is an ARGOS position  $v_{\text{obs}}$  with coordinates  $(x_{\text{obs}}, y_{\text{obs}})$  and a corresponding true position  $v_{\text{true}}$ . The 2 positions are connected through the positioning errors  $\varepsilon_x$  and  $\varepsilon_y$ :

$$\begin{aligned}\varepsilon_x &= X_{\text{obs}} - X_{\text{true}} \\ \varepsilon_y &= Y_{\text{obs}} - Y_{\text{true}}\end{aligned}\quad (\text{A1})$$

The probability that a given point  $(a, b)$  is the true position corresponding to  $v_{\text{obs}}$  is given as:

$$\begin{aligned}P(X_{\text{true}} = a \wedge Y_{\text{true}} = b) &= P(X_{\text{obs}} - \varepsilon_x = a \wedge Y_{\text{obs}} - \varepsilon_y = b) = \\ P(\varepsilon_x = X_{\text{obs}} - a \wedge \varepsilon_y = Y_{\text{obs}} - b)\end{aligned}\quad (\text{A2})$$

The probability in Eq. (A2) is described by the bivariate Gaussian distribution if  $\varepsilon_x$  and  $\varepsilon_y$  are normally distributed:

$$P(\varepsilon_x, \varepsilon_y) = \frac{1}{2\pi\sigma_x\sigma_y\sqrt{1-\rho^2}} e^{-\frac{z}{2(1-\rho^2)}}$$

where

$$z = \frac{(\varepsilon_x - \mu_x)^2}{\sigma_x^2} + \frac{(\varepsilon_y - \mu_y)^2}{\sigma_y^2} - \frac{2\rho(\varepsilon_x - \mu_x)(\varepsilon_y - \mu_y)}{\sigma_x\sigma_y} \quad \text{and} \quad \rho = \frac{\sigma_{xy}}{\sigma_x\sigma_y}$$

$\mu_x$  and  $\mu_y$  are mean errors,  $\sigma_x$  and  $\sigma_y$  are standard deviations and  $\rho$  the correlation between  $\varepsilon_x$  and  $\varepsilon_y$ . It is reasonable to assume that errors on longitude and latitude are uncorrelated ( $\rho = 0$ ) and that mean error is zero (observed positions are not displaced from true positions in a systematic direction). These assumptions are supported by results of Vincent et al. (2002). Given these assumption, the above reduces to:

$$P(\varepsilon_x, \varepsilon_y) = \frac{1}{2\pi\sigma_x\sigma_y} e^{-\frac{1}{2}\left[\frac{\varepsilon_x^2}{\sigma_x^2} + \frac{\varepsilon_y^2}{\sigma_y^2}\right]}\quad (\text{A3})$$

In order to calculate the probability that the true position  $v_{\text{true}}$  corresponding to the observed position  $v_{\text{obs}}$  is located inside some square  $A$  (or rectangle), we introduce the standardized cumulated probability function for the uncorrelated bivariate Gaussian distribution  $\Phi$  ( $\rho = 0$ ;  $\mu_x = \mu_y = 0$ ;  $\sigma_x = \sigma_y = 1$ ):

$$\Phi(a, b) = P(x < a \wedge y < b) = \frac{1}{2\pi} \int_{-\infty}^a \int_{-\infty}^b e^{-\frac{x^2+y^2}{2}} dx dy\quad (\text{A4})$$

As for the univariate distribution, this integral cannot be solved analytically, and one is forced to resort to polynomial approximation or numerical methods. The approximation given by Divgi (1979) was used in this example. The probability we are looking for is the probability that the true position  $v_{\text{true}}$  corresponding to the observed position  $v_{\text{obs}}$  with coordinates  $(x_{\text{obs}}, y_{\text{obs}})$  is located inside a rectangle  $A$  with corners  $(a_1, b_1)$  and  $(a_2, b_2)$ . This is given as:

$$\begin{aligned}P(v_{\text{true}} \in A) &= \frac{1}{2\pi\sigma_x\sigma_y} \int_{b_1}^{b_2} \int_{a_1}^{a_2} e^{-\frac{1}{2}\left[\left(\frac{x-x_{\text{obs}}}{\sigma_x}\right)^2 + \left(\frac{y-y_{\text{obs}}}{\sigma_y}\right)^2\right]} dx dy = \\ &\Phi\left(\frac{a_1 - x_{\text{obs}}}{\sigma_x}, \frac{b_1 - y_{\text{obs}}}{\sigma_y}\right) + \Phi\left(\frac{a_2 - x_{\text{obs}}}{\sigma_x}, \frac{b_2 - y_{\text{obs}}}{\sigma_y}\right) - \left[\Phi\left(\frac{a_1 - x_{\text{obs}}}{\sigma_x}, \frac{b_2 - y_{\text{obs}}}{\sigma_y}\right) + \Phi\left(\frac{a_2 - x_{\text{obs}}}{\sigma_x}, \frac{b_1 - y_{\text{obs}}}{\sigma_y}\right)\right]\end{aligned}\quad (\text{A5})$$

Eq. (A5) gives the probability that a single position belongs in the area  $A$ . By combining the results for all positions received we can calculate the probability that the number of true positions inside a given grid cell is larger than zero ( $P(n_A > 0)$ ). This probability is easily calculated from the joint probability that none of the  $N$  positions in the dataset belongs to  $A$  ( $P(n_A = 0)$ ):

$$P(n_A > 0) = 1 - P(n_A = 0) = 1 - \prod_{i=1}^N (1 - P(v_i \in A))\quad (\text{A6})$$

A second useful parameter is the most likely number of true positions in  $A$ . This figure equals the mean number of true positions in  $A$  in the hypothetical situation where the entire data collection is repeated several times.  $E(n_A)$  is given as:

$$E(n_A) = \sum_{i=1}^N P(v_i \in A)\quad (\text{A7})$$